Electronic Properties of Particle-Counting Diamonds. I. Photoconductivity

L. A. Vermeulen and F. R. N. Nabarro

Phil. Trans. R. Soc. Lond. A 1967 **262**, 251-276
doi: 10.1098/rsta.1967.0050

ELECTRONIC PROPERTIES OF PARTICLE-COUNTING DIAMONDS

I. PHOTOCONDUCTIVITY

By L. A. VERMEULEN and F. R. N. NABARRO
Department of Physics, University of the Witwatersrand, Johannesburg, South Africa

(*Communicated by F. C. Frank, F.R.S.—Received* 11 *October* 1966)

CONTENTS

	PAGE
1. Introduction	251
2. Previous work	251
3. The apparatus	253
4. Photoconductivity experiments	254
4·1. The dark current	254
4·2. Photoconduction	254
5. A preliminary discussion of the photoconductivity	264
6. Formal theory of the model proposed for the counting diamonds	270
7. Conclusion	274
References	278

An account is given of an experimental investigation into the photoconductivity of particle-counting diamonds at room temperature and at 80 °K. Photoconduction spectra were obtained in the range 2500 to 200 nm which are typical of type I a diamonds. The room temperature spectra are characterized by a system of eight photoconduction peaks. The peaks are attributed to the intrinsic absorption, the thermal decomposition of excitons and the excitation of three levels in the forbidden energy gap at 0·85, 1·45 and 2·2 eV from the valence band. This model is consistent with the known electro-optical properties of type I a diamonds. The model is formulated mathematically and formally shown to predict the observed photoconduction responses of the diamonds to certain characteristic illuminations.

1. Introduction

This paper describes the photoconduction spectra of particle-counting diamonds. The spectra are typical of type I a diamonds. Diamonds of this type contain nitrogen predominantly in a non-paramagnetic platelet form (Dyer, Raal, Du Preez & Loubser (1965)). The effect of illumination on the counting properties of these diamonds will be discussed in the succeeding paper.

2. Previous work

The published work on the electrical conduction properties of insulating diamonds is not extensive. The relevant data will now be summarized:

Photoconductivity in diamond was first observed by Gudden & Pohl in 1920. They found that:

(1) The photoconduction spectra of two of their diamonds were characterized by a pronounced minimum at about 310 nm. These diamonds were subsequently classified by Robertson, Fox & Martin (1934) as type I.

(2) These type I diamonds were photoconductive when illuminated with red light only after previous illumination with light of energy greater than about 2·1 eV.

(3) Although the diamonds were not normally photoconductive when illuminated with red light, the presence of this light during illumination with blue or ultraviolet light enhanced the photocurrent due to the latter excitation.

The spectra obtained by Gudden & Pohl (1920) and Robertson *et al.* (1934) are reproduced in figures 1 and 2 respectively.

Some or all of these observations have been confirmed by Levi (1922), Robertson *et al.* (1934), Taylor (1956), Urlau (1960), Nahum & Halperin (1962, 1963) and Halperin & Nahum (1962).

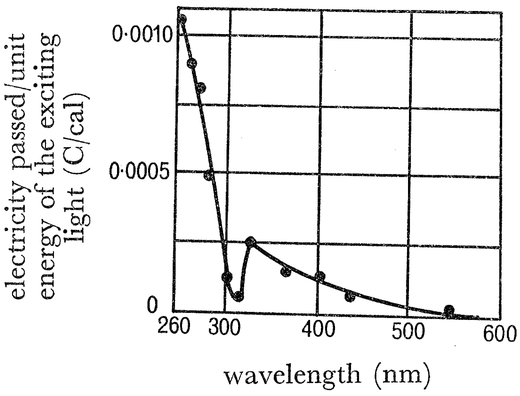

FIGURE 1. The photoconduction spectrum of a diamond (Gudden & Pohl 1920).

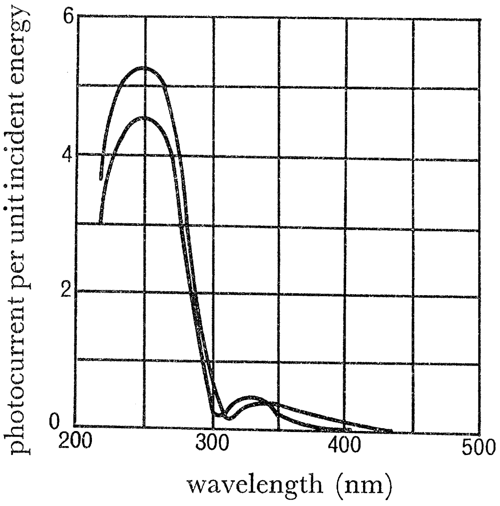

FIGURE 2. The photoconduction spectra of two type I diamonds (Robertson *et al.* 1934).

Pant (1944) and Willardson & Danielson (1950) did not measure spectra, but confirmed the observations (2) and (3) of Gudden & Pohl.

Champion & Dale (1956) investigated the red-light photocurrent as a function of the temperature.

The influence of monochromatic light in the spectral range from 1·8 to 3·5 eV on the rate of decay of the space-charge field in counting diamonds was studied by Elmgren & Hudson (1962).

Photoconduction spectra of type I a diamonds have recently been measured by Konorova, Sorokina & Shevchenko (1965), whose results are in good agreement with the present work.

The photo-Hall effect in insulating diamonds during illumination with ultraviolet light was measured by Lenz (1925) and Klick & Maurer (1951). The authors agree that under these conditions the charge carriers are electrons with a mobility of the order of $10^3\,\mathrm{cm^2\,V^{-1}\,s^{-1}}$. Redfield (1954) found both *n*- and *p*-type diamonds in his study of the temperature dependence of the Hall mobility of the charge carriers in illuminated diamonds.

The temperature dependence of the electrical conductivity of insulating diamonds was measured by Pogodaev (1961), who found activation energies of 0·96, 1·4 and 2·3 eV, in good agreement with Urlau, Logie & Nabarro (1961).

3. The apparatus

The photocurrents were measured with a Keithley model 610 electrometer, having a sensitivity of 10^{-13} A full scale, with an accuracy of 4 % on the most sensitive ranges. The output of the electrometer was connected to a pen recorder.

Monochromatic illumination was obtained from a Zeiss M4Q11 monochromator. It utilizes two light sources in covering the wavelength range from 2500 to 200 nm, namely a tungsten filament lamp and a pressurized deuterium lamp, both driven with d.c. stabilized power supplies. The power output from the monochromator using the tungsten filament lamp was measured with a thermopile. That of the deuterium lamp and the dispersion of the monochromator were supplied by the manufacturers. These curves were used in the normalization of the photoconduction spectra.

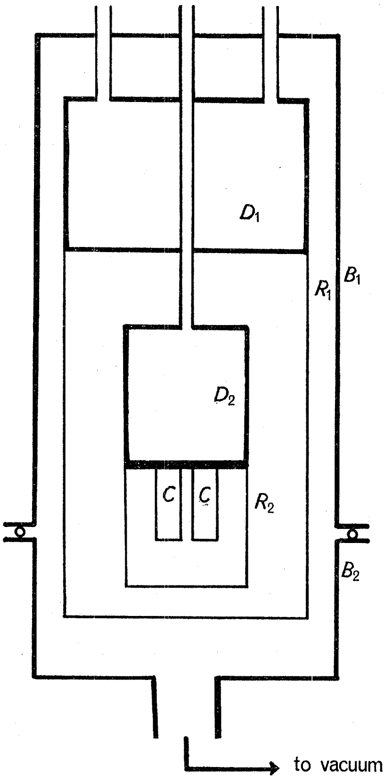

Figure 3. The optical cryostat.

An optical cryostat (figure 3) was built so that the photoconductivity of the diamonds could be measured both at room and at liquid nitrogen temperatures.

Two sections of a brass cylinder, B_1 and B_2, are provided with flanges for an O-ring seal. Two copper Dewar vessels are mounted into the upper section, B_1. They are fitted with copper radiation shields R_1 and R_2. The Dewar vessels are thermally insulated from B_1 by means of thin-walled german silver tubing, also used for filling them with liquid nitrogen.

The section B_1 is provided with a quartz window through which a diamond clamped in the crystal holder C can be illuminated, and a viewing window to ensure proper focusing of the light. The crystal holder is in thermal contact with the liquid nitrogen in D_2 through being mounted on a heavy copper disk soldered into the bottom of D_2. One of the electrodes from C is a heavy copper rod which is thermally anchored to the copper disk. The radiation shields are provided with inlet and exit ports for the exciting light.

The assembled apparatus was mounted directly on to a diffusion pump provided with suitable fittings, and evacuated to a pressure of less than 0·1 μmHg.

The temperature of the crystal holder was measured (in the dark) to be within 10 degC of that of liquid nitrogen.

The monochromator was placed as close as possible to the quartz window of the cryostat to ensure maximum illumination. The quartz window was fitted with a blackened light pipe and the viewing window with a shutter so that the diamonds could be kept either in darkness or illuminated only with the desired light.

The signal-carrying lead from the crystal holder in the cryostat was soldered on to a vacuum lead-through around which was externally mounted a plug that mated directly with the input of the current-measuring electrometer. This elimination of flexible co-axial cable between the electrometer and the cryostat ensured a minimum of interference and other noise.

The diamonds were small octahedral crystals of the order of 1 mm³. They were selected for their particle-counting properties from a 200 carat sample of gem sand from the Sierra Leone diamond mines. They were provided with electrical contacts consisting of thin films of an amalgam of mercury, indium and thallium painted on to a pair of parallel crystal faces. The contacts were non-rectifying, and under certain conditions they were also ohmic.

4. PHOTOCONDUCTIVITY EXPERIMENTS

4·1. *The dark current*

A measurable dark current was found to persist in most of the counting diamonds after application of an electric field. This was so whether the diamonds were provided with contacts or not.

That insulating diamonds are non-rectifying with the contacts used here is demonstrated in table 1.

TABLE 1. THE CURRENT–VOLTAGE CHARACTERISTIC OF DIAMOND G5

voltage (V)	steady forward current (10^{-14} A)	steady reverse current (10^{-14} A)
90	1·3	1·3
180	3·0	2·9
270	4·9	4·6
360	6·8	6·8
450	9·2	9·1
630	14·0	14·0
720	17·2	16·7
810	20·0	19·8

4·2. *Photoconduction*

We define a photoresponse to be the variation of the photocurrent as a function of the time during steady illumination of a diamond, the applied field being held constant.

Typical photoresponses to infrared, red and green light are shown in figure 4. The basic features are:

(1) The photoresponse to infrared light is purely transient, the whole development taking place within 5 or 6 min, depending on the wavelength and intensity of the light. This will be called the *X* response.

(2) The response to red light is also transient, but of several hours' duration. This will be called the *R* response.

(3) In the response to green light and light of higher energies the photocurrent usually passes through a minimum before levelling off to a steady value. Sometimes the photocurrent simply increases to a steady value. This will be called the *G* response.

There are always qualitative and easily recognizable differences between the *X*, *R* and *G* photoresponses. The *X* and *R* responses are not seen unless the diamond has previously been illuminated with *G* light. This will be called the Gudden–Pohl effect, since it was first discovered by them (Gudden & Pohl 1920).

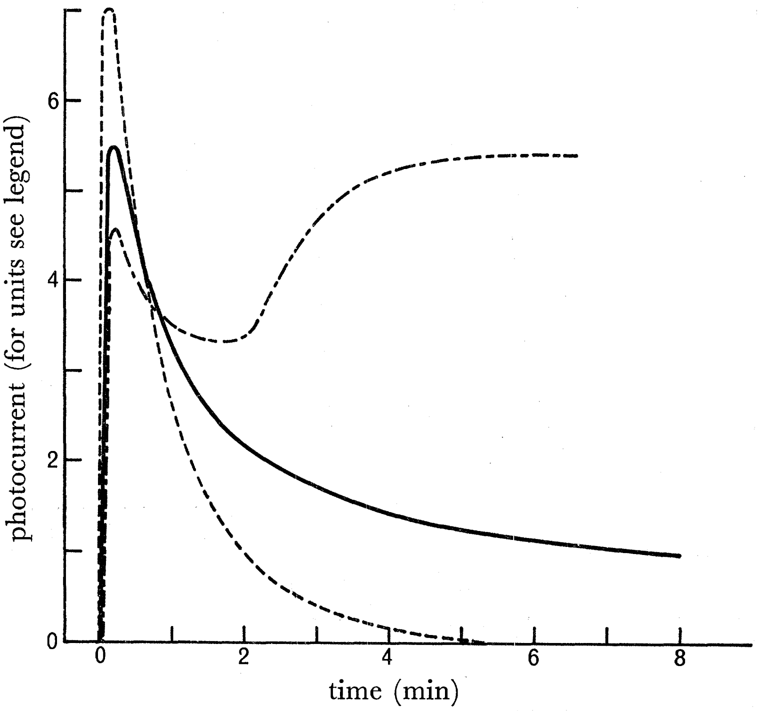

Figure 4. The photoconductive response of particle-counting diamonds to various monochromatic illuminations. (– – –, 1200 nm and 10^{-13} A/div.; ——, 600 nm and 10^{-13} A/div.; – — –, 450 nm and 10^{-11} A/div.).

Since the photocurrent depends both on time and on the history of the diamond, it was decided to study the photoconduction spectra by a continuous method. The available spectrum was swept through by coupling a small electric motor to the spindle of the monochromator, the photocurrent being continuously recorded.

A photoconduction spectrum obtained by this method, using each of the lamps in the monochromator in turn over its full range of emission, is shown in figure 5. We recognize provisionally a system of seven peaks in the spectrum, which are labelled *X*, *R*, *G*, *G′*, *R′*, *E* and *I*. The peaks *G*, *G′* and *R′* are common to both spectra in the region of overlap between 500 and 300 nm. The wavelength scale was obtained from the monochromator. It is approximately linear in energy.

The reliability of the method may be assessed by comparing the spectra obtained in this way with those of Gudden & Pohl (1920) and Robertson *et al.* (1934) shown in figures 1 and 2. The minimum at about 310 nm is a feature of the spectra reported by these authors and of the spectrum obtained here with the deuterium lamp.

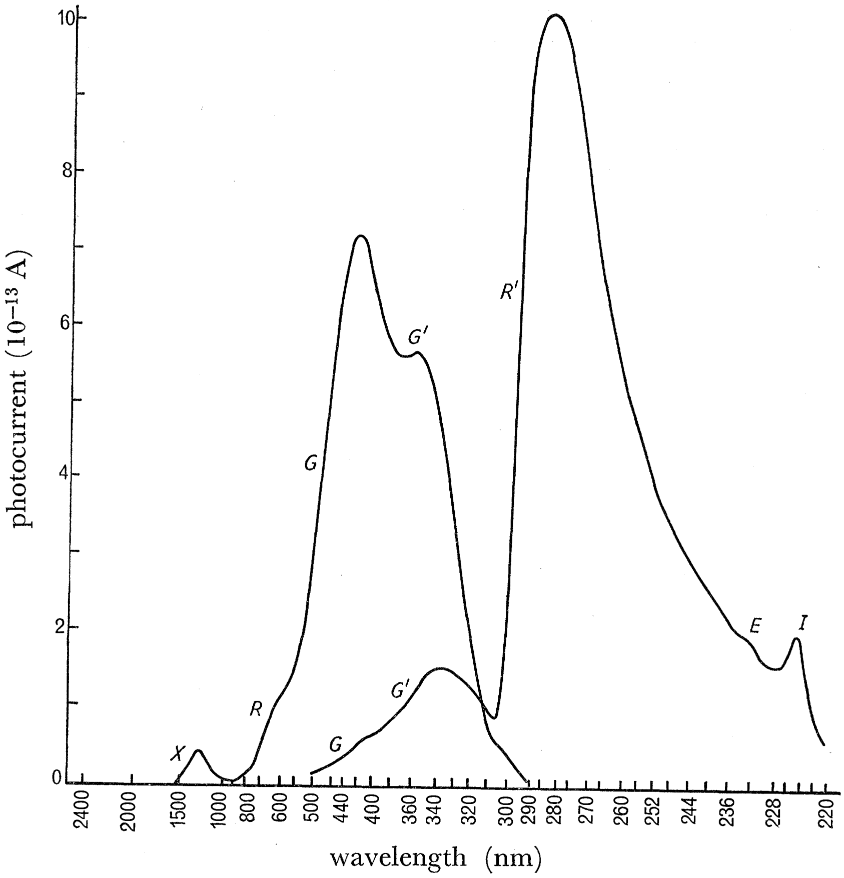

FIGURE 5. The photoconduction spectrum of diamond G5 at room temperature.

The peaks *X*, *R*, *G*, *E* and *I* may also be recognized in the photoconduction spectra of type I diamonds measured by Nahum & Halperin (1962, 1963) and Halperin & Nahum (1962), *R* and *G* in the spectra of Taylor (1956), *X*, *R*, *G′*, *R′* and *I* in the spectra of Urlau *et al.* (1961), *R′* and *I* in the spectra of Konorova *et al.* (1965).

There is also almost perfect agreement between the positions of the minima in our measurements of the complicated photoconduction spectra of type IIb diamonds and those of Hardy, Smith & Taylor (1962), which is further evidence for the reliability of the method.

The shape of the photoconduction spectra may depend on:

(1) the electric field strength,

(2) the sweep rate,

PHILOSOPHICAL TRANSACTIONS OF THE ROYAL SOCIETY A MATHEMATICAL, PHYSICAL & ENGINEERING SCIENCES

(3) the direction of the sweep—whether from low to high energy or vice versa,
(4) the monochromator slit width,
(5) the temperature,
(6) the orientation.

Quantitative reproducibility of the photoconduction spectra may be obtained when all of the experimental variables (1) to (6) are held constant with the electric field strength less than about 6000 V/cm. The reproducibility may be almost exact in measurements corresponding to a full-scale deflexion of 10^{-12} A, after five or six spectra have been recorded.

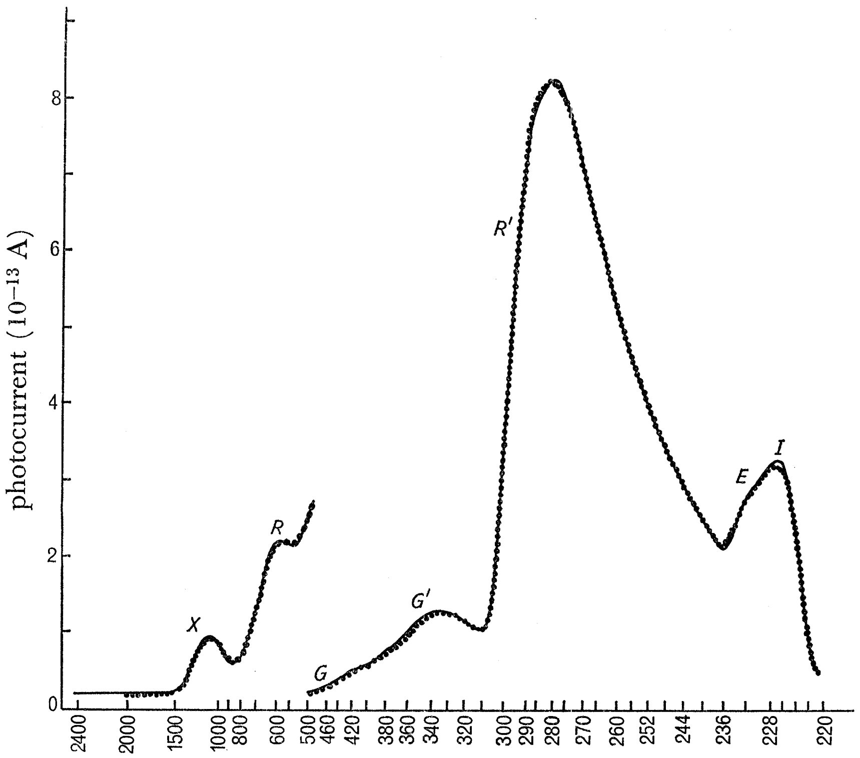

FIGURE 6. Two reference spectra from diamond G5 at room temperature are superposed to demonstrate the reproducibility of a photoconduction spectrum when the diamond is in the standard photoconductive state. The spectrum is typical of type Ia diamonds.

This is shown in figure 6, where two successive spectra are superposed. The discontinuity at 500 nm is due to switching of the light sources in the monochromator.

We call the state of a diamond in which it yields a fully reproducible photoconduction spectrum a standard photoconductive state. The photoconduction spectrum obtained from a diamond in a standard state will be called a reference spectrum.

The photoconduction spectra were found to depend on some of the experimental variables listed above. The influence of these variables will now be discussed.

(1) *The electric field strength.* The photoconduction spectra were most easily measured with field strengths in the range 900 to 6000 V/cm, usually 1800. With lower field strengths the

currents were small and the resolution poor. With higher strengths the apparatus became unstable.

It was expected that the introduction of the carrier mobility concept would greatly facilitate the interpretation of the observations. The concept is valid for diamond at room temperatures at field strengths below 10^4 V/cm.

(2) *The sweep rate.* The sweep rates used in the present work were between 0·52 and 0·0087 eV/min. It was possible to increase the sweep rate further, but this resulted in a loss of resolution. Decreasing the sweep rate improved the resolution and shifted the characteristic features of the spectrum to slightly shorter wavelengths. Sweep rates less than 0·13 eV/min resulted in the suppression of the *X*-peak in the infrared. These effects are demonstrated in figure 7, where the reference photoconduction spectra obtained at sweep rates of 0·52, 0·13 and 0·017 eV/min are shown. The *X* peak is most strongly developed by the fastest sweep, but is entirely suppressed by the slowest sweep. Low sweep rates cause enhancement of the peaks *E* and *I* in the ultraviolet and the sharper definition of *R*.

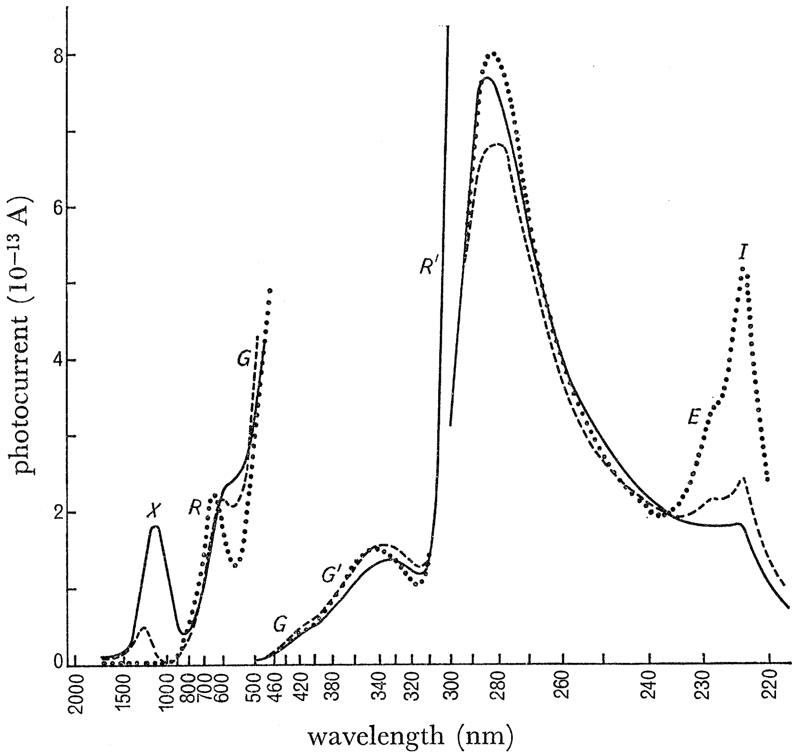

FIGURE 7. Reference photoconduction spectra obtained at three different forward sweep rates from diamond G11 at room temperature. The *X* peak is suppressed at low sweep rates. The discontinuity at *ca.* 300 nm is due to a change of scale to $3{\cdot}0 \times 10^{-13}$ A/div.

(3) *The direction of the sweep.* Most information is gained when the direction of the sweep is forward, i.e. from low to high energy. All of the peaks *X, R, G, G', R', E* and *I* are developed in the forward sweep. When the sweep is reversed, the *X* peak is suppressed. Apart from small shifts of the characteristic features of the spectrum to longer wavelengths and quantitative differences in the magnitudes of the peaks, the spectra are otherwise similar. The peaks *R, G, G', R', E* and *I* are readily identifiable in both spectra.

(4) *The monochromator slit width.* This parameter governs simultaneously the output intensity of the monochromator and the band width of the light. It was found convenient to optimize the slit width in accordance with the requirements that the slit be kept as narrow as possible and the magnitude of the largest peak in the photoconduction spectrum just correspond to a full scale deflexion.

(5) *Temperature.* An optical cryostat was built so that the photoconduction spectra of diamonds could be studied both at room temperature and at 80 °K. Quantitative differences between the reference spectra obtained at these two temperatures were always apparent.

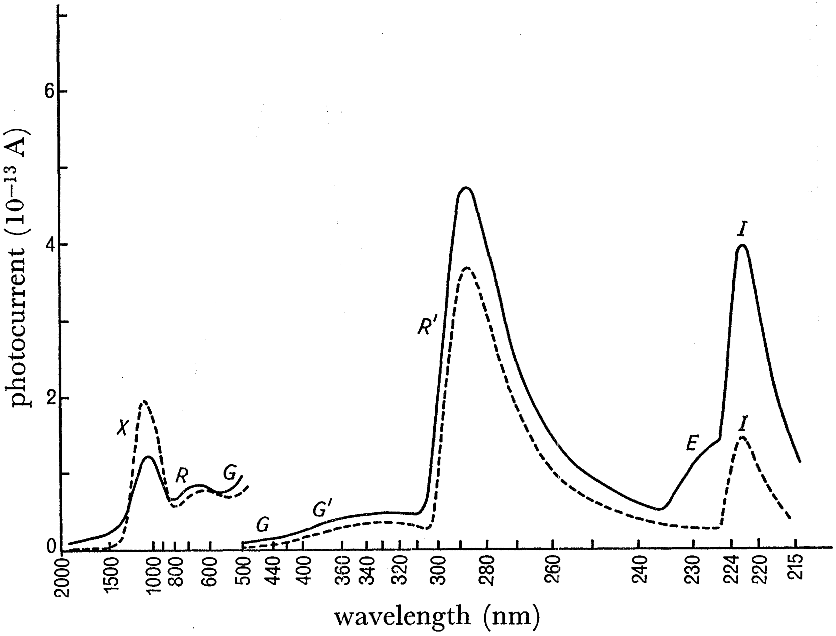

FIGURE 8. The reference photoconduction spectra of diamond G15 at room temperature (—) and at 80 °K (-----).

In some cases the peaks were larger at the low temperature and in other cases the reverse was true. The characteristic features were displaced to shorter wavelengths in the photoconduction spectra obtained at liquid nitrogen temperature. The peak *E* was suppressed at the low temperature. *A* photoconduction spectrum demonstrating this effect is shown in figure 8.

(6) *The orientation.* In some cases the peaks *E* and *I* are not developed in a photoconduction spectrum. A typical example is shown in figure 9. In these cases it was found, especially when the photocurrent is still appreciable at 225 nm, that the photocurrent decreases rapidly, almost discontinuously, for wavelengths shorter than 224 nm. The spectrum is otherwise ordinary and the peaks *X*, *R*, *G*, *G'*, *R'* can always be recognized at the usual wavelengths.

In a number of diamonds specifically studied for the effect it was always possible, by rotating the diamond in the crystal holder so as to present different faces to the illumination but still keep the same faces in contact with the electrodes, to find a position in which the peaks *E* and *I* were developed. This is demonstrated in figure 10, where three reference photoconduction spectra of diamond G7 are reproduced. The other experimental conditions are identical in the three cases. In position 6 the diamond is favourably oriented for the development of the peaks *E* and *I*.

The shape of the large peak *R′* when the diamond is in position 3 suggests that this peak normally conceals a further peak which we will call *X′*.

The occurrence of this peak *X′* has an important bearing on the interpretation of the results. Its direct observation by the technique of orienting the diamond was possible with other specimens. An indirect demonstration of its existence will be given below in § 5.

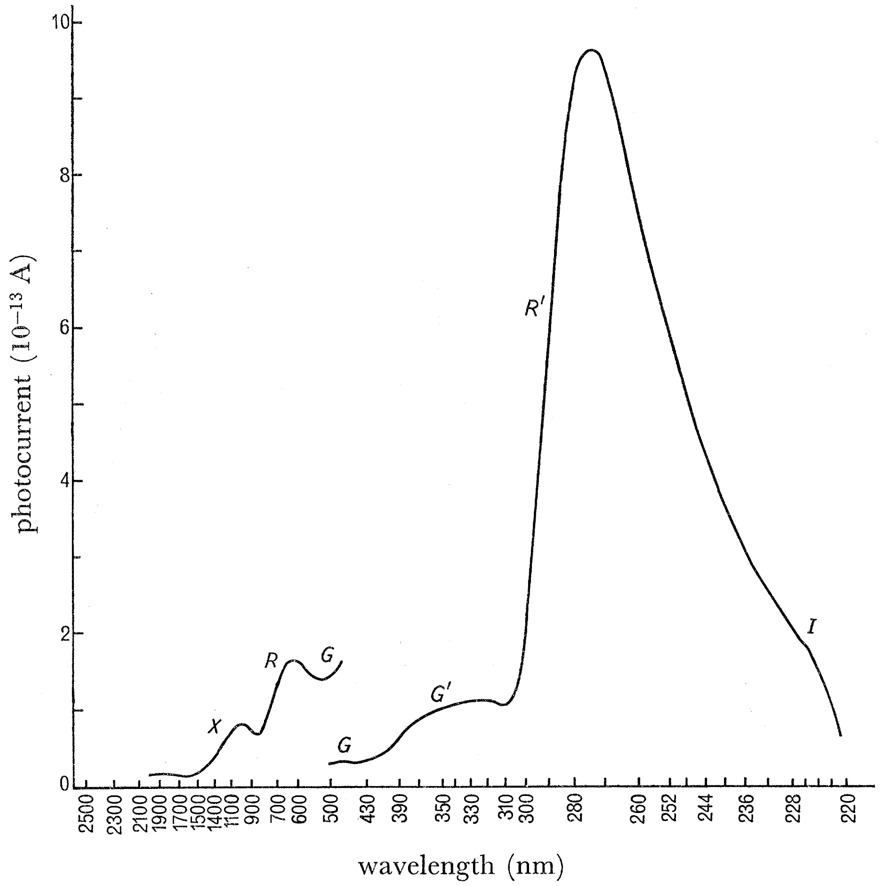

FIGURE 9. An example of a photoconduction spectrum of a type I a diamond in which the peaks *E* and *I* are not developed.

The results lead to the following assumption. The room temperature photoconduction spectra of the counting diamonds, which were all of type I, are in general characterized by a system of eight peaks, varying degrees of development being obtained with the individuals of this type.

The photoconduction spectra of twenty-seven counting diamonds were studied at room and liquid nitrogen temperatures. For purposes of comparison, the photoconduction spectra of numbers of known type I a, type I b, type II a and type II b diamonds were also studied. It was found that:

(1) The photoconduction spectra of diamonds are characteristic of their type.

(2) The photoconduction spectra of the counting diamonds were all similar. The peaks

X, *R*, *G*, *G′*, *R′* were identifiable in all of them. The spectra were similar to those obtained from known type Ia diamonds.

(3) There was evidence for the existence of the peak *X′* in the photoconduction spectra of nine of the counting diamonds.

(4) The peaks *E* and *I* were also found in the photoconduction spectra obtained from one of the type IIa diamonds. They were obtained only in one out of four cases when the diamonds were in the form of polished blocks.

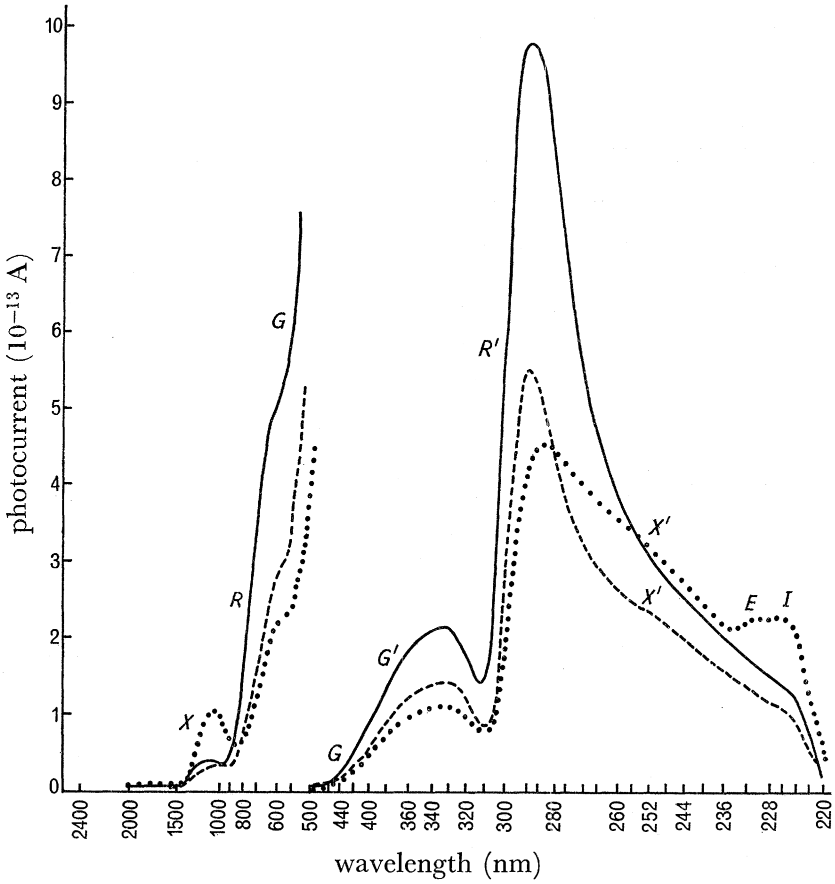

FIGURE 10. Reference photoconduction spectra of diamond G7 at room temperature. The experimental conditions are identical except that the diamond has been rotated between the electrodes so as to present different faces to the illumination. The shape of the large peak *R′* suggests that it conceals a peak called *X′*. In position 6 the diamond is favourably oriented for the development of the peaks *E* and *I*.

Because of (2) it is believed that the counting diamonds all contain the same defects—the defects that make them type Ia. Because of (4) it is believed that the peaks *E* and *I* are a general property of diamond, which may be masked by surface effects.

The long-wavelength limits of the peaks in the photoconduction spectra define the energies of levels in the forbidden energy gap. These critical wavelengths and the corresponding energies are tabulated below.

The critical wavelengths and energies could not be more accurately determined from the present work.

None of the spectra so far reported has been corrected for variation in the intensity of illumination with wavelength. The output power of the monochromator may be described as follows:

(*a*) With the tungsten filament lamp it has a maximum at 1·2 μm with the power decreasing rapidly with decreasing wavelength.

(*b*) With the deuterium lamp the power increases monotonically as the wavelength decreases from 350 to 220 nm.

(*c*) The emission spectrum of either lamp is perfectly line-free in the range over which it was utilized.

Table 2. Critical wavelengths and energies associated with the photoconduction spectra of the counting diamonds

peak	critical wavelength (nm)	critical energy (eV)
X	1450 ± 100	0·85 ± 0·1
R	850 ± 20	1·46 ± 0·06
G	560 ± 10	2·2 ± 0·1
G′	380 ± 10	3·3 ± 0·1
R′	306 ± 3	4·05 ± 0·07
X′	260 ± 10	4·8 ± 0·2
E	236 ± 2	5·25 ± 0·07
I	225 ± 1	5·52 ± 0·03

A photoconduction spectrum of diamond G 3 which has been corrected for variation in the intensity of the incident illumination is shown in figure 11. Also shown in the same figure is the uncorrected spectrum plotted out on a linear energy scale. It is seen that the long wavelength limits of the peaks are only slightly affected by the normalization. However, the strongly developed peak *R* in the unnormalized spectrum is almost suppressed when the curve is corrected for variation in the intensity of the incident illumination. Since the existence of the peak *R* was clearly established, the unnormalized spectra are used, both to save labour and to facilitate identification of the *R* peak.

The current-voltage characteristics of the diamonds when illuminated with red, blue and ultraviolet light were measured. The results are shown in figure 12.

A similar measurement with infrared illumination was impossible, because of the transient nature of the response to this light. Measurements with red light were difficult but possible, because the photoresponse, although transient, decays to zero over many hours. The values of the current, which are plotted here against voltage, are those obtained 1 h after the application of the voltage when the rate of decrease of the current is small. In the case of the characteristics obtained with blue and ultraviolet light, the value of the eventual steady current is plotted against the applied voltage.

The diamonds were non-rectifying during illumination with any light.

The measurements shown in figure 12 were repeatable, and gave the same results if the applied voltage was increased stepwise from zero up to the highest value or decreased from the highest value to the lowest value used.

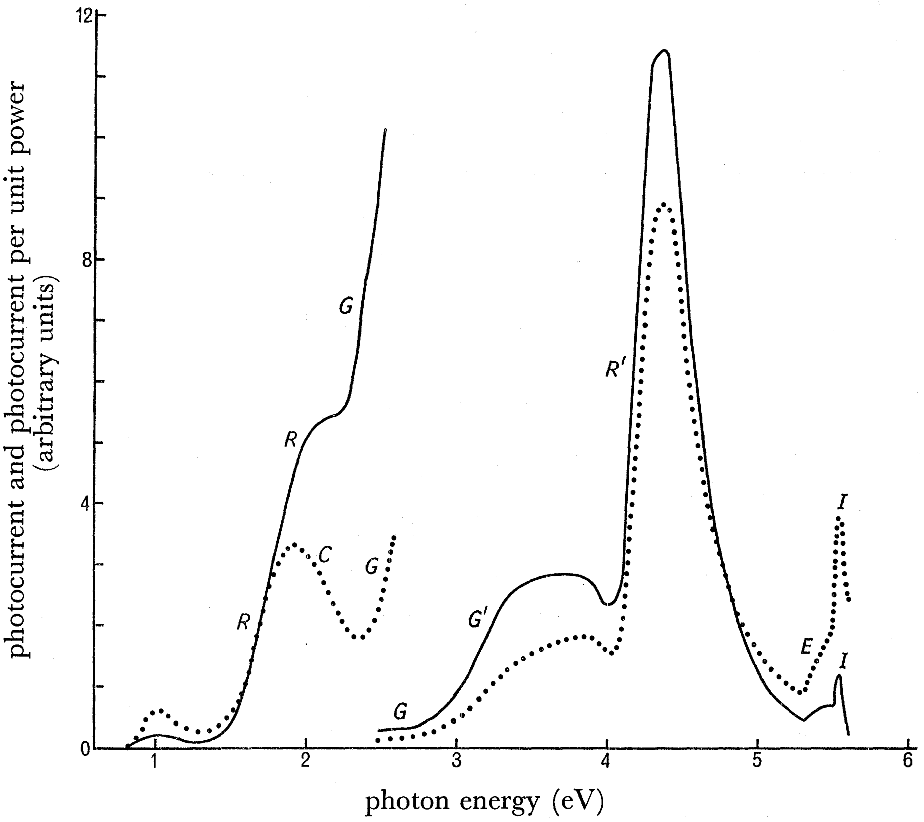

FIGURE 11. The photoconduction spectrum of diamond G3 at room temperature; ——, corrected for variations in the intensity of illumination; ......, uncorrected but transferred from the recorder trace to a linear energy scale.

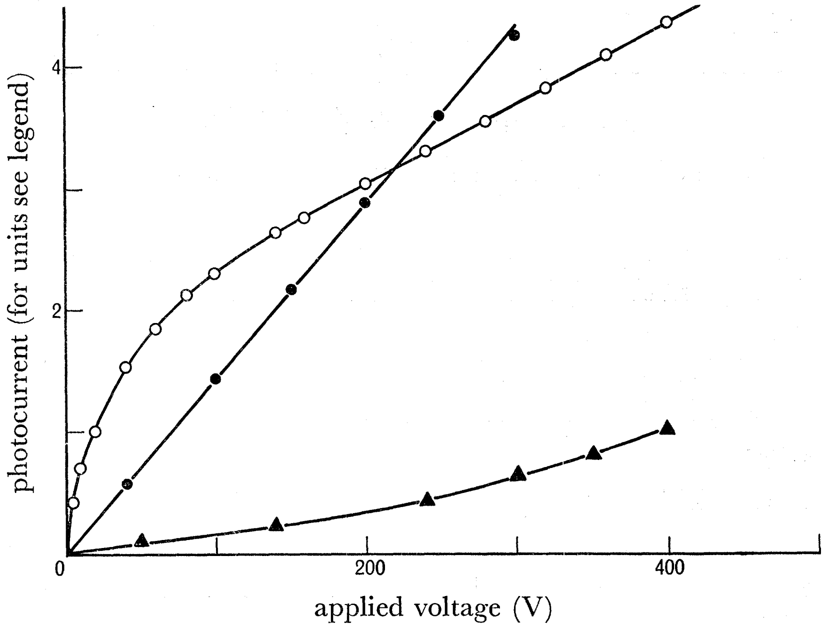

FIGURE 12. The current-voltage characteristics of diamond G14b at room temperature. ▲, During illumination with *R* light (600 nm) (scale, 10^{-12} A); ○, during illumination with *G* light (420 nm) (scale, 10^{-12} A); ●, during illumination with u.v. (276 nm) (scale, 10^{-11} A).

5. A preliminary discussion of the photoconductivity

The photoconduction spectra of counting diamonds are characterized by the occurrence of eight peaks, which have been called *X*, *R*, *G*, *G*′, *R*′, *X*′, *E* and *I*. The latter two, which are not always developed, will now be interpreted.

Their dependence on the state of the surface is indicated by the following facts:

(*a*) The peaks are hardly ever seen in the spectra obtained from polished diamonds, and in the only polished block in which they were seen initially they disappeared after radiation damage;

(*b*) in the case of some of the counting diamonds the development of these peaks depended on the crystal orientation.

As was pointed out by Mott & Gurney (1940, p. 104), the photoconduction falls off at energies greater than the intrinsic energy. At these energies the absorption coefficient may be as high as $10^6\,\mathrm{cm}^{-1}$. Such high absorption is accompanied by fast recombination, especially at recombination centres on the surface of the crystal. The photocurrent therefore decreases when the absorption becomes too high, because the radiation enters only a surface film of the material, and only this surface film can be made conducting. In the presence of fast recombination the strong absorption compensates only partly for the thinness of the film.

Following Halperin & Nahum (1962), who observed both the suppression of photoconductivity and the enhancement of luminescence at low temperature at 236 nm, we attribute the peak *E* to the thermal decomposition of excitons. The thermal ionization of an excited level could also explain the observations.

The peak I which has its maximum at about 5·5 eV is the intrinsic peak, since 5·5 eV is the width of the forbidden energy gap.

The further discussion is concerned with the explanation of the peaks *X*, *R*, *G*, *G*′, *R*′ and *X*′ in terms of isolated levels in the forbidden energy gap. These peaks are due to the direct excitation of levels in the forbidden energy gap, as shown by the fact that peaks are still developed at 80 °K. We notice that the energies (table 2) satisfy the relations

$$X+X' \simeq R+R' \simeq G+G' \simeq 5{\cdot}5\,\mathrm{eV},$$

the width of the forbidden energy gap. This suggests a three-level model such as that shown in figure 13.

In this model the *X*, *R* and *G* peaks are due to excitation of electrons from the valence band to the *X*, *R* and *G* levels, and the *G*′, *R*′ and *X*′ peaks to the complementary transitions from the levels to the conduction band.

There are eight possible three-level models of the forbidden energy gap, since each transition may be exchanged with its complementary transition.

It is now necessary:

(i) to confirm the model by showing that a coupling exists between the peaks and their complements;

(ii) to examine whether or not a three-level model can account for the observed photoresponses described in §4.2;

(iii) to examine the consistency of the model with other known electro-optical effects in diamond; and

(iv) to select the correct three-level model from the possible eight.

We first discuss point (i).

The strongest evidence we have for the coupling of the levels is the fact that the energies associated with the peaks add up to the width of the forbidden energy gap. The following observations, which do not by themselves prove the coupling, are consistent with it.

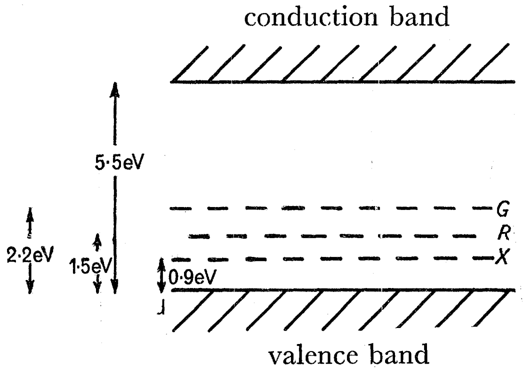

Figure 13. A three-level model of the forbidden energy gap of diamond.

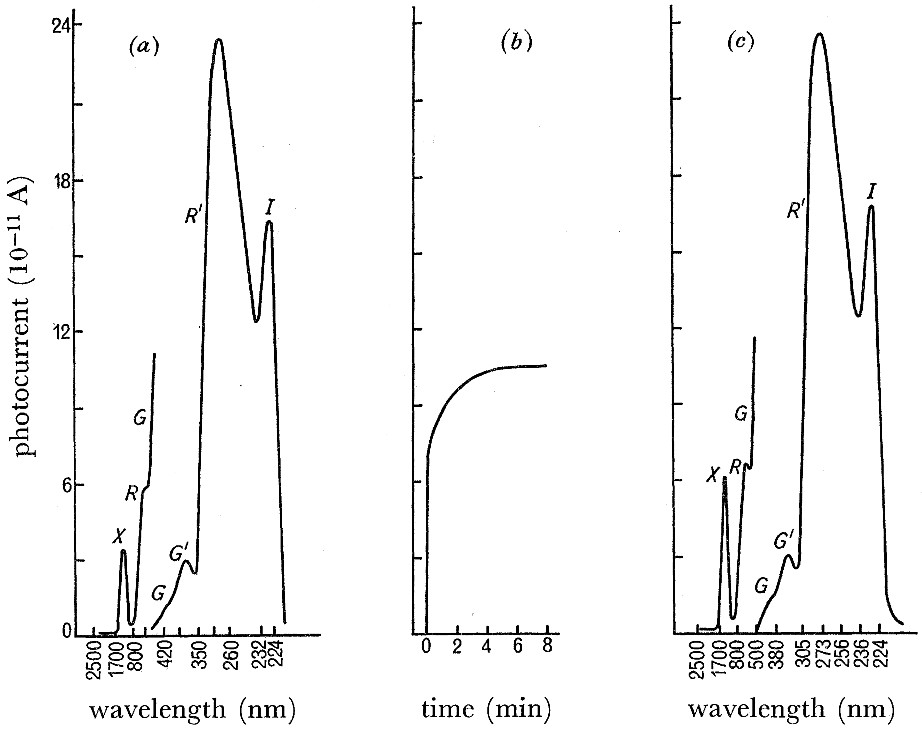

Figure 14. The coupling of X and X'. (*a*) Reference spectrum; (*b*) X' response; (*c*) spectrum after illumination with X' light (2600 Å)

In figure 14 the reference spectrum of G5 is followed by its response to X' light. In the first spectrum obtained after X' response has been measured, the X peak has been considerably enhanced.

According to the model of figure 13, the X' light removed electrons from some of the states comprising the X level to the conduction band. These electrons were then redistributed among all three levels, leaving fewer electrons in the X level than there were in the standard photoconductive state. The X peak, whose magnitude is roughly proportional to the number of empty states in the X level, is enhanced. A strict proportionality cannot be expected because of space charge limitations.

The effect also provides an indirect demonstration for the existence of the X' peak, which is normally obscured by the large neighbouring peak R' in the photoconduction spectra of type I diamonds.

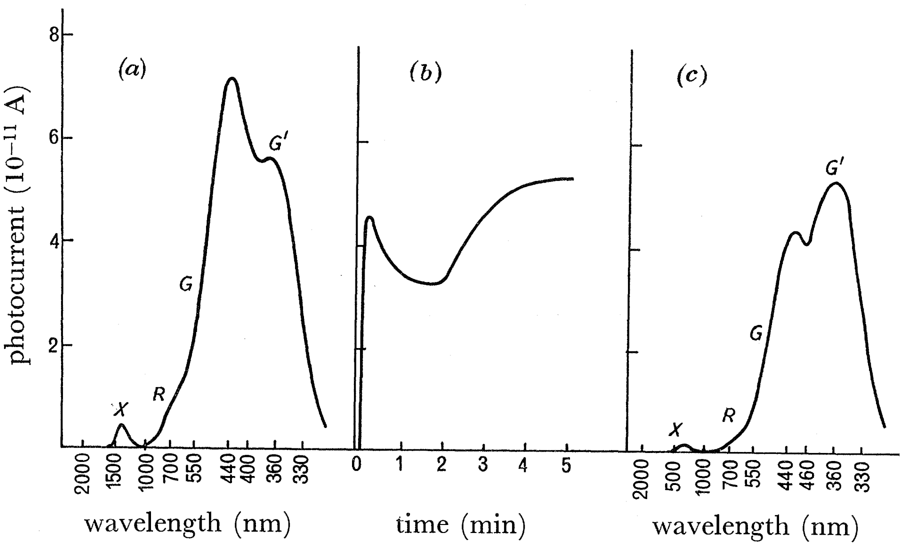

FIGURE 15. The coupling of G and G'. Diamond G 5 at room temperature. (*a*) Reference spectrum; (*b*) G response (4500 Å); (*c*) spectrum after illumination with G light.

The coupling between G and G' is shown in figure 15. The reference spectrum, obtained by use of the tungsten lamp only, is followed by the response to G light. In the first spectrum obtained after the response to G light it is seen that the G' peak is enhanced. In terms of the model of figure 13, G light tends to populate the G level through excitation of electrons from the valence band to the level. Accordingly, the G' peak is enhanced.

The coupling between R and R' has not been so convincingly demonstrated (figure 16). It is found that the R' peak grows only by a few percent after illumination with R light, and vice versa.

We now turn to the photoresponses shown in figure 4. The main features were discussed in § 4·2.

We shall show that the model of figure 13 can qualitatively explain all the observations. We assume that the Fermi level in the dark lies above the R level, so that the R level is more than half full and the X level is almost completely filled. The experimental evidence indicates that this is so. Absorption corresponding to the X and R peaks in the photoconduction spectrum is normally undetectably small. In the photoconduction spectra the intensity of the light at these points is more than 100 times that at the complementary peaks, yet the photoconduction at the complementary peaks X' and R' is larger. This indicates that the R level is in general much more than half full. This information, taken in conjunction with the measurement of Gudden & Pohl (1920), reduces the number of acceptable three-level models. Four of these are shown in figure 17. The remaining four are the mirror images of the four shown. The prediction of each as regards excitation with green light is summarized in the figure. The model of figure 17 (iv) and its mirror image are the only three-level models which explain the result of Gudden and Pohl (verified by Pant (1944) and Willardson & Danielson (1950)) that the diamonds are not photoconducting when illuminated with either infrared or red light, unless they have previously been excited with light of energy greater than about 2·1 eV, i.e. *G* light.

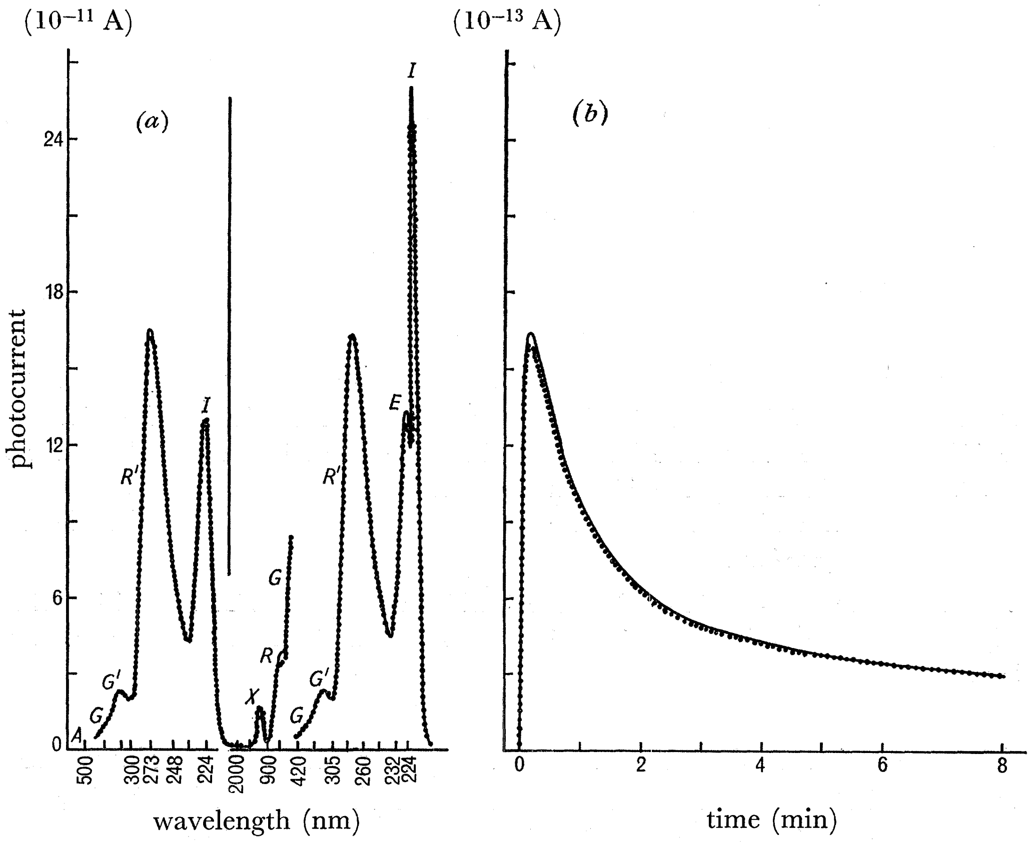

FIGURE 16. The photoresponse of diamond G5 to *R* light. (*a*) The curve on the right is the reference spectrum, that on the left is the spectrum obtained after recording the *R* response; (*b*) *R* response (6000 Å). The figure also demonstrates the reproducibility of the measurements. Two curves are superposed everywhere in (*a*) and (*b*).

Illumination with *X* light can have no effect if the *X* level is already fully occupied in the dark. If the crystal is illuminated with *G* light, electrons can be excited from the valence band to the *G* level. The resulting holes contribute to the photocurrent for a short time until they are annihilated through recombination with electrons from the *X*, *R* and *G* levels. If the light is switched off, this recombination proceeds until all the holes have been annihilated and the crystal is again in a stable state. Recombination is fast (the lifetimes of free charge carriers in diamond are of the order 10^{-8} s, Pearlstein & Sutton 1950), and has always been observed to be completed in a time shorter than the time constant of the apparatus. The net effect of the illumination has been to transfer electrons from the *X* level to the *R* and *G* levels, thereby leaving some of the states in the *X* level unoccupied. If now the crystal is re-illuminated with *X* light, it will photoconduct, because electrons can now be excited from the valence band to the unoccupied states in the *X* level by the *X* light. This is the Gudden–Pohl effect.

In terms of figure 17 (iv) the explanation of the *X* and *R* responses is as follows: during continued illumination with *X* light, holes will continuously be annihilated through recombination with electrons from the *X*, *R* and *G* levels. The *X* level will eventually become filled, because it is continuously under excitation and the number of free holes decreases because of the continuous recombination from *R* and *G*. The diamond ceases to conduct during continuous illumination with *X* light. The explanation of the *R* response is similar.

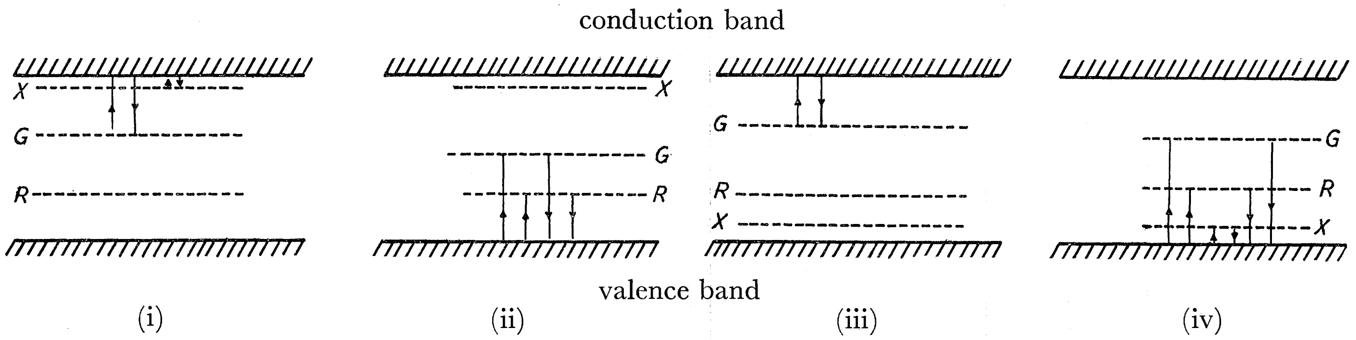

(i) *G* light cannot stimulate the *R* response if both the *X* and *R* are transient.

(ii) *G* light can stimulate the R response but not the *X*-response if both *X* and *R* responses are transient.

(iii) *G* light cannot stimulate the *X* and *R* responses.

(iv) *G* light can stimulat both the *X* and *R* re- sponses when they ar transient.

FIGURE 17. Four possible three-level models of the forbidden energy gap. The transitions shown are the only ones possible under excitation with *G* light when the *X* and *R* photoresponses are transient.

As experimental evidence that the *X* level is completely filled after prolonged exposure to *X* light we note, first, that all attempts to measure the photo-Hall effect during illumination with infrared or red light have so far failed (R. G. Farrer 1964, private communication). A more sensitive demonstration involves the reversal of the applied field.

In figure 18 are shown the reference spectrum of diamond C7 and the first spectrum obtained after reversal of the applied field. The *X* peak is twenty-seven times larger when the field is reversed. The effective field strength is now equal to the applied field plus the previous space charge field. (With repeated cycling, the diamond polarizes in the opposite direction and the reference spectrum is eventually recovered.) This enhanced sensitivity was used in the following series of experiments:

(i) the diamond was put into the standard state and the *X* response was observed;

(ii) the *X* light was switched off and the voltage reversed;

(iii) the *X* light was switched on again.

In (iii) the conditions are most favourable for the observation of the *X* response if any of the states in the *X* level are vacant. The experiment was carried out with a number of diamonds on a scale where a deflexion corresponding to 10^{-15} A could easily have been detected. In every case the result was zero.

The observation that simultaneous illumination with red light enhances the photoconductivity due to ultraviolet light is also explained in terms of figure 17 (iv). The red light replenishes the *R* level with electrons as they are removed by the ultraviolet light.

It is impossible, with the use of non-rectifying contacts, to decide purely on the basis of photoconductivity between a given level configuration and its mirror image. The photo-Hall effect distinguishes between these two models. It is only necessary to fix the position of one of the levels relative to either of the bands. Farrer (1964, private communication) found that the counting diamonds are *p* type during illumination with light of energy 2·2 eV. The most likely model is therefore that of figure 17·4, and not its mirror image. This is consistent with the findings of Lenz (1925) and Klick & Maurer (1951) that the diamonds

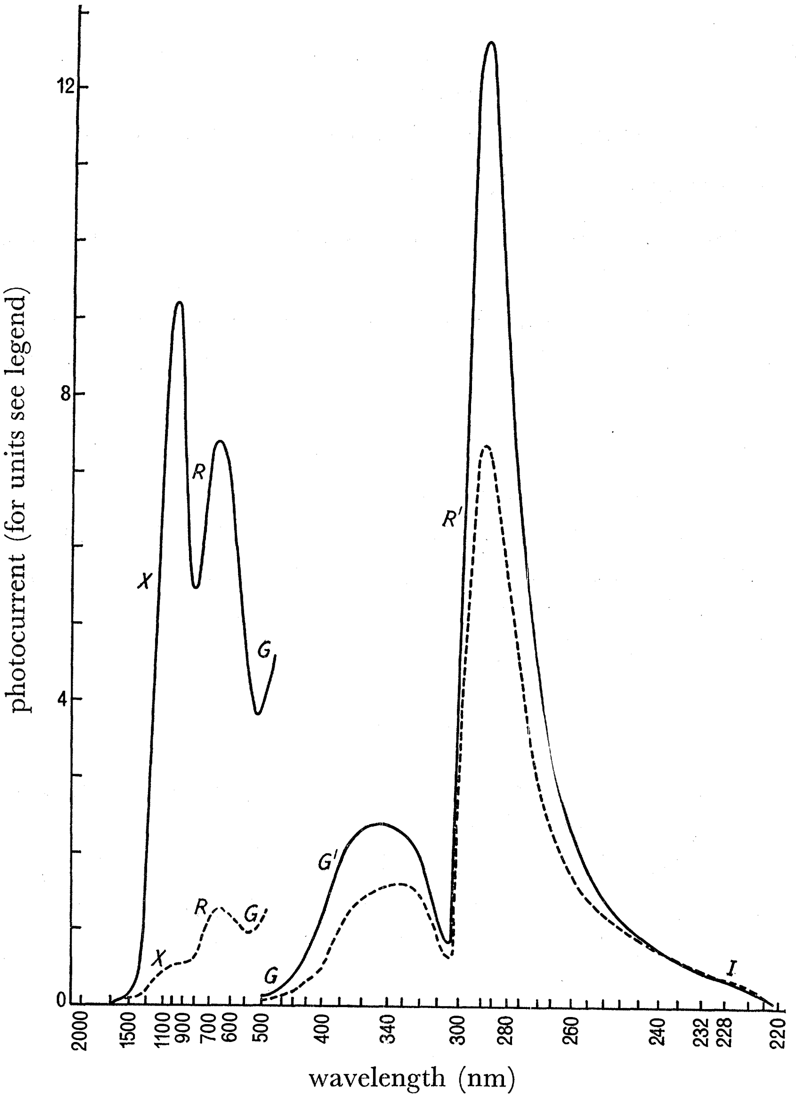

FIGURE 18. The effect of reversing the electric field applied to diamond C 7; – – – – –, reference spectrum (Scale: $\times 10^{-13}$ A/div.); ——, first spectrum after reversal of the applied field (scale, 3×10^{-13} A/div.).

are n type during illumination with about 4 eV light, which is energetic enough to excite electrons from some of the levels to the conduction band.

The activation energies are in good agreement with those found by Urlau *et al.* (1961) and Pogodaev (1961). Urlau *et al.* proposed the model of figure 17 (iii), which is inconsistent with some of the data now reported.

6. FORMAL THEORY OF THE MODEL PROPOSED FOR THE COUNTING DIAMONDS

Three ideas are fundamental to the following discussion. These are:

(*a*) that Ohm's law is approximately valid;

(*b*) that the free charge carrier density is zero when the diamonds of this type are in darkness;

(*c*) that the standard photoconductive state is a long-lived state corresponding to a standard non-equilibrium population configuration of the levels in the forbidden energy gap.

As evidence for (*a*) we note, first, that the diamonds were non-rectifying when provided with the contacts described in § 3. Secondly, the current-voltage characteristics are approximately ohmic at 180 V when the diamonds are in the dark (table 1), or illuminated with red (600 nm) or blue (420 nm) or ultra violet (276 nm) light (see figure 12). It will therefore be assumed that the free charge carrier density may always be put into correspondence with the photocurrent through a relation such as

$$\sigma = e(n\mu_n + p\mu_p),$$

where σ is the conductivity, e the electronic charge, n and p are the densities of free electrons and holes, and μ_n and μ_p are their mobilities.

To justify (*b*) we note that the dark current in a field strength of 1 kV/cm is of the order 10^{-14} A or less. Assuming that the free carriers are all holes, we have $\sigma = pe\mu_p$. With a hole mobility of about $10^3\,\mathrm{cm^2\,V^{-1}\,s^{-1}}$, (Austin & Wolfe 1956; Wedepohl 1957) we find for diamonds of the order of $1\,\mathrm{mm^3}$ that

$$\begin{aligned} p &\approx 10\,\mathrm{cm^{-3}} \\ &= 10^{-2}\,\mathrm{mm^{-3}}. \end{aligned}$$

It is therefore a fair approximation to say that the free carrier density is zero in the dark.

The evidence for (*c*) is provided by:

(i) the almost permanent memory of the diamonds;

(ii) the reproducibility of the reference photoconduction spectrum;

(iii) the reproducibility with which a response can be measured.

In connexion with (i) we note that the photodepolarization of a diamond may still be detected months after the crystal has been polarized at room temperature. It is possible to polarize a diamond as in the counting experiments (described in the following paper II), or by measuring its photoconductivity, to take it out of the crystal holder and leave it in a drawer for over a year, to put it back in the crystal holder and still measure a photocurrent without an applied field. This is not a photovoltaic effect, because a diamond can be depolarized by 'blacking it out' as defined in § 4 of paper II. The photodepolarization spectrum in counting diamonds is in all cases similar to, but on a smaller scale than, the usual reference spectra.

On the basis of a conductivity of 10^{-14} $(\Omega\,\mathrm{cm})^{-1}$ the relaxation time of diamond may be computed from the formula $\tau_R = \epsilon_r \epsilon_0/\sigma$ to be only about 50 s. This suggests that most of the current measured in the dark flows on the surface and not through the bulk.

Points (ii) and (iii) are demonstrated in figure 16. The preparation of the crystal is shown in figure 16 (*a*), and two responses in figure 16 (*b*). Two curves are superposed everywhere in figure 16 from the point *A* in the bottom left-hand corner of figure 16 (*a*) to the end of the response in figure 16 (*b*). Even in the original tracings it is difficult to recognize that two curves are superposed except at points such as *R* and *I*.

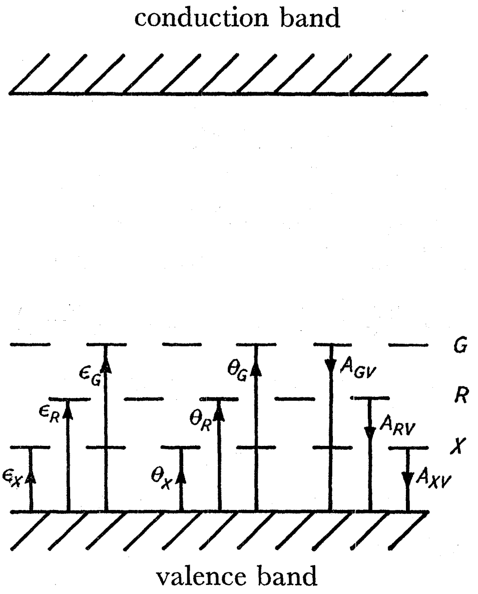

FIGURE 19. The three-level model showing the possible transitions during excitation with *G* light.

It will now be demonstrated formally that a three-level model in principle yields solutions for the free carrier density which vary in time as do the observed *X*, *R* and *G* responses.

The model is shown in figure 19.

Suppose that the *G*, *R* and *X* levels contain *G*, *R* and *X* states per unit volume, of which *g*, *r* and *x* are occupied by electrons.

If the sample is illuminated with *G* light, all of the levels are accessible to the electrons in the valence band. Electrons are excited from the band edge to the *G* level and from deeper in the valence band to the *R* and *X* levels.

In the figure, the optical and thermal excitations are denoted by ϵ_i and θ_i respectively, and the recombination transition probabilities by A_{ij}.

During illumination with G light the model may be formulated as follows:

$$\mathrm{d}g/\mathrm{d}t = \epsilon_G(G-g) - A_{GV}\,gp + \theta_G(G-g), \tag{1}$$

$$\mathrm{d}r/\mathrm{d}t = \epsilon_R(R-r) - A_{RV}\,rp + \theta_R(R-r), \tag{2}$$

$$\mathrm{d}x/\mathrm{d}t = \epsilon_X(X-x) - A_{XV}\,xp + \theta_X(X-x), \tag{3}$$

$$\begin{aligned}\mathrm{d}p/\mathrm{d}t = {} & \epsilon_X(X-x) + \theta_X(X-x) + \epsilon_R(R-r) + \theta_R(R-r) \\ & + \epsilon_G(G-g) + \theta_G(G-g) - A_{GV}\,gp - A_{RV}\,rp - A_{XV}\,xp.\end{aligned} \tag{4}$$

The ϵ_i and θ_i, and X, R and G are constants, and the time-dependent variables are x, r and g.

We can estimate θ_X from the equation

$$\theta_X(X-x) = \nu(X-x)\exp(-E_X/kT), \tag{5}$$

where ν is an attempt-to-escape frequency for holes bound to the X centres. The maximum values of ν is about the frequency of crystal vibrations, say $10^{13}\,\mathrm{s}^{-1}$. The Boltzmann factor, $\exp(-E_X/kT)$, represents the probability of an electron in the valence band having the necessary energy E_X to be excited to the X level.

Substituting numerical values we find that the rate of thermal excitation from the valence band to the X level can be at most $10^{-2}(X-x)$. This might be appreciable if the density of unoccupied X-states is large. For the R and G levels the rates are

$$10^{-12}(R-r) \quad \text{and} \quad 10^{-38}(G-g),$$

respectively.

The recombination transition probability A_{XV} is given by

$$A_{XV}\,xp = S_{XP}\,v_h\,xp, \tag{6}$$

where S_{XP} is the capture cross-section of occupied states in the X level for holes in the valence band with thermal velocity v_h. The other trapping or recombination transition probabilities are similarly interpreted.

The effect of the light is represented by the quantities ϵ_i. Thus the rate of optical excitation per unit volume from the valence band to the G level is given by the equation

$$\epsilon_G(G-g) = Iq(\lambda)\,\mu(\lambda), \tag{7}$$

where I is the intensity of the light, $q(\lambda)$ is the number of free carriers created per unit energy of the absorbed light and $\mu(\lambda)$ is the absorption coefficient for light of wavelength λ.

Let the populations in the standard photoconductive state be g_0, r_0, x_0 and p_0. We then have

$$\left.\begin{aligned}&\epsilon_G = \epsilon_R = \epsilon_X = 0\\ \text{and}\quad &\mathrm{d}g/\mathrm{d}t = \mathrm{d}r/\mathrm{d}t = \mathrm{d}x/\mathrm{d}t = 0.\end{aligned}\right\} \tag{8}$$

The experimentally determined condition that $p_0 \simeq 0$ implies that $x \simeq X$ and $r \simeq R$.

We obtain an approximate solution by linearizing the equations (1) to (4). Put

$$g = g_0 + \gamma, \quad r = r_0 + \rho, \quad x = x_0 + \xi, \quad p = p_0 + \pi, \tag{9}$$

where γ, ρ, ξ and π are the deviations in the populations from the standard state. Then

$$\mathrm{d}g/\mathrm{d}t = \mathrm{d}\gamma/\mathrm{d}t, \quad \mathrm{d}r/\mathrm{d}t = \mathrm{d}\rho/\mathrm{d}t, \quad \mathrm{d}x/\mathrm{d}t = \mathrm{d}\xi/\mathrm{d}t, \quad \mathrm{d}p/\mathrm{d}t = \mathrm{d}\pi/\mathrm{d}t. \tag{10}$$

We obtain

$$\left.\begin{aligned}
\mathrm{d}\gamma/\mathrm{d}t &= \epsilon_{GG}(G-g_0)-(\epsilon_{GG}+\theta_G+A_{GV}p_0)\,\gamma-A_{GV}\,g_0\,\pi,\\
\mathrm{d}\rho/\mathrm{d}t &= \epsilon_{RG}(R-r_0)-(\epsilon_{RG}+\theta_R+A_{RV}p_0)\,\rho-A_{RV}\,r_0\,\pi,\\
\mathrm{d}\xi/\mathrm{d}t &= \epsilon_{XG}(X-x_0)-(\epsilon_{XG}+\theta_X+A_{XV}p_0)\,\xi-A_{XV}\,x_0\,\pi,\\
\mathrm{d}\pi/\mathrm{d}t &= \epsilon_{GG}(G-g_0)+\epsilon_{RG}(R-r_0)+\epsilon_{XG}(X-x_0)-(\epsilon_{GG}+\theta_G+A_{GV}p_0)\,\gamma\\
&\quad -(\epsilon_{RG}+\theta_R+A_{RV}p_0)\,\rho-(\epsilon_{XG}+\theta_X+A_{XV}p_0)\,\xi-(A_{GV}\,g_0+A_{RV}\,r_0+A_{XV}\,x_0)\,\pi.
\end{aligned}\right\}\quad(11)$$

We have added the extra subscript, G, to the ϵ's because we are dealing specifically with the case of excitation with G light.

By the conservation of charge

$$\pi = \gamma+\rho+\xi. \quad (12)$$

Using (12) to eliminate π in (11) we obtain

$$\left.\begin{aligned}
(\mathrm{D}+e_1+a_1)\,\gamma+a_1\,\rho+a_1\,\xi &= \epsilon_{GG}(G-g_0)\\
a_2\,\gamma+(\mathrm{D}+e_2+a_2)\,\rho+a_2\,\xi &= \epsilon_{RG}(R-r_0)\\
a_3\,\gamma+a_3\,\rho+(\mathrm{D}+e_3+a_3)\,\xi &= \epsilon_{XG}(X-x_0).
\end{aligned}\right\}\quad(13)$$

Here $\mathrm{D}=\mathrm{d}/\mathrm{d}t$,

$$\begin{aligned}
e_1 &= \epsilon_{GG}+\theta_G+A_{GV}\,p_0, & a_1 &= A_{GV}\,g_0,\\
e_2 &= \epsilon_{RG}+\theta_R+A_{RV}\,p_0, & a_2 &= A_{RV}\,r_0,\\
e_3 &= \epsilon_{XG}+\theta_X+A_{XV}\,p_0, & a_3 &= A_{XV}\,x_0.
\end{aligned}$$

Equations (13) can be written in the form

$$\left.\begin{aligned}
\frac{\mathrm{d}^3\gamma}{\mathrm{d}t^3}+K_G\frac{\mathrm{d}^2\gamma}{\mathrm{d}t^2}+L_G\frac{\mathrm{d}\gamma}{\mathrm{d}t}+M_G\,\gamma &= S_{\gamma G},\\
\frac{\mathrm{d}^3\rho}{\mathrm{d}t^3}+K_G\frac{\mathrm{d}^2\rho}{\mathrm{d}t^2}+L_G\frac{\mathrm{d}\rho}{\mathrm{d}t}+M_G\,\rho &= S_{\rho G},\\
\frac{\mathrm{d}^3\xi}{\mathrm{d}t^3}+K_G\frac{\mathrm{d}^2\xi}{\mathrm{d}t^2}+L_G\frac{\mathrm{d}\xi}{\mathrm{d}t}+M_G\,\xi &= S_{\xi G}.
\end{aligned}\right\}\quad(14)$$

From (14) and (12) we obtain for the free carrier density

$$\frac{\mathrm{d}^3\pi}{\mathrm{d}t^3}+K_G\frac{\mathrm{d}^2\pi}{\mathrm{d}t^2}+L_G\frac{\mathrm{d}\pi}{\mathrm{d}t}+M_G\,\pi = S_{\pi G}. \quad (15)$$

The general solution of this equation is of the form

$$\pi = \pi_{\infty G}+\pi_{1G}\,\mathrm{e}^{\lambda_{1G}t}+\pi_{2G}\,\mathrm{e}^{\lambda_{2G}t}+\pi_{3G}\,\mathrm{e}^{\lambda_{3G}t}, \quad (16)$$

where $\pi_{\infty G}$ is the particular integral given by

$$\pi_{\infty G} = S_{\pi G}/M_G > 0.$$

The quantities π_{1G}, π_{2G} and π_{3G} are constants to be determined by the boundary conditions.

The λ's are given by the determinantal equation

$$\begin{vmatrix}
\lambda+e_1+a_1 & a_1 & a_1\\
a_2 & \lambda+e_2+a_2 & a_2\\
a_3 & a_3 & \lambda+e_3+a_3
\end{vmatrix} = 0 \quad \text{or} \quad \lambda^3+K_G\lambda^2+L_G\lambda+M_G = 0, \quad (17)$$

which defines K_G, L_G and M_G.

It is readily shown (Vermeulen 1967) that the roots of the auxiliary equation (17) are real and negative. We see therefore that

$$\pi_G \to \pi_{\infty G} > 0 \quad \text{as} \quad t \to \infty.$$

When π has been determined the values of γ, ρ and ξ may be found from the first three of equations (10) together with the condition that these quantities are zero at the beginning of the illumination. Since the equations are linear these three quantities may be made small in comparison with the corresponding densities of occupied states g, r and x.

The aim of this paragraph is accomplished if a function of the form (16) can be found which will vary in time as the G response.

The empirical function

$$\pi = 171 - 147\,\mathrm{e}^{-0\cdot315t} + 3573\,\mathrm{e}^{-3\cdot77t} - 3597\,\mathrm{e}^{-4\cdot02t} \tag{18}$$

and the experimentally obtained G response are shown together in figure 20.

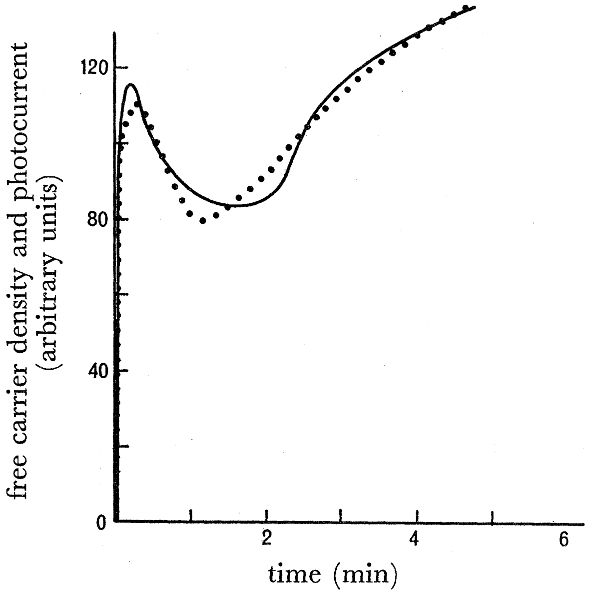

FIGURE 20. A comparison of the time dependence of the free carrier density as predicted by equation (18) (·····) and the experimentally obtained G response (——).

We identify the fastest constant with the X level because the X response is the most fleeting of the responses, and the longest time constant with the G level because a permanent photocurrent is obtained only during excitation with G light.

The R response is obtained from the theory by putting $\epsilon_G = 0$ everywhere in the above. Similarly the X response is obtained by putting both ϵ_G and ϵ_R equal to zero.

The three-level theory developed in this paragraph will be applied to the counting properties of diamond in the succeeding paper.

7. CONCLUSION

In the course of the present investigation, numbers of diamonds of all the major types, i.e. type Ia, type Ib, type IIa and type IIb in the classification recently proposed by Dyer *et al.* (1965) were examined. The photoconduction spectra reported here are typical of the type Ia diamonds. These diamonds contain nitrogen in a non-paramagnetic, platelet form.

Since photoconductivity is a more sensitive test than optical absorption, we classify all our particle-counting diamonds as type Ia, whereas some of them would previously have been called type II, because they are weakly transparent to light of a wavelength (2800 Å) shorter than 3000 Å.

We do not claim that type II diamonds are non-counters, but we have found, contrary to Champion (1952, 1953; Champion & Kennedy 1965) that good counting diamonds are often of type Ia.

The levels we have postulated here are those whose excitation involves the creation of free charge carriers. The positions of the levels are then defined by the long-wavelength limits of the photoconduction peaks. Absorption systems such as the 4150 Å system, G.R.I., the 5032 Å system, etc., are due to the excitation of electrons from levels, not necessarily the same levels, to excited states within the forbidden energy gap. That is to say, excitation of these systems does not involve the creation of free charge carriers, unless the excited state is so close to the band edge that ionization can take place thermally. Such absorption systems may also be detected in photoconductivity when the measurements are carried out on a sufficiently fine scale at low temperatures. An absorption system is then revealed as a sequence of sharp minima against a background of photoconduction. The minima correspond exactly with the absorption peaks in the optical absorption spectrum, and arise from the absorption of light without the creation of free charge carriers. This was first shown by Halperin & Nahum (1962) in the case of the 4150 Å system and confirmed by the present authors for this system and the G.R.I. system.

Konorova *et al.* (1965) have correlated the large photoconduction peak, called R' in the present work, with nitrogen impurity in diamond. We agree with this identification and indeed believe this peak to be correlated specifically with nitrogen platelets, since it occurs only in type Ia diamonds and not in type Ib in which the nitrogen is atomically dispersed and paramagnetic.

This research was sponsored by Industrial Distributors (1946) Ltd, and the diamonds were supplied by the Diamond Research Laboratory, Johannesburg. It is a pleasure to acknowledge many helpful discussions with Dr F. R. L. Schöning, Dr P. T. Wedepohl, D. L. Allinson, R. G. Farrer and E. Wessels of the Department of Physics of the University of the Witwatersrand, and Dr H. B. Dyer, Dr F. A. Raal, Dr L. du Preez and M. Holland of the Diamond Research Laboratory.

References

Austin, I. G. & Wolfe, R. 1956 *Proc. Phys. Soc.* B **69**, 329.
Champion, F. C. 1952 *Proc. Phys. Soc.* B **65**, 465.
Champion, F. C. 1953 *Proc. Roy Soc.* A **220**, 485.
Champion, F. C. & Dale, B. 1956 *Proc. Roy. Soc.* A **234**, 419.
Champion, F. C. & Kennedy, P. J. 1965 *Physical properties of diamond* (Ed. R. Berman) Oxford: Clarendon Press.
Dyer, H. B., Raal, F. A., Du Preez, L. & Loubser, J. H. N. 1965 *Phil. Mag.* **11**, 763.
Elmgren, J. A. & Hudson, D. E. 1962 *Phys. Rev.* **128**, 1044.

Gudden, B. & Pohl, R. W. 1920 *Z. Phys.* **3**, 123.

Halperin, A. & Nahum, J. 1962 *Luminescence in organic and inorganic materials* (Ed. Kallmann, H. P. & Spruch, G. M.). New York: Wiley.

Hardy, J. R., Smith, S. D. & Taylor, W. 1962 *Proc. Int. Conf. on Physics of Semiconductors, Exeter.* London: Institute of Physics and the Physical Society.

Klick, C. C. & Maurer, R. J. 1951 *Phys. Rev.* **81**, 124.

Konorova, E. A., Sorokina, L. A. & Shevchenko, S. A. 1965 *Soviet Phys. Solid St.* **7**, 876.

Lenz, H. 1925 *Annln. Phys.* **77**, 449.

Levi, M. 1922 *Trans. Roy. Soc. Canad.* **16**, 243.

Mott, N. F. & Gurney, R. W. 1940 *Electronic processes in ionic crystals.* Oxford: Clarendon Press.

Nahum, J. & Halperin, A. 1962 *J. Phys. Chem. Solids* **23**, 345.

Nahum, J. & Halperin, A. 1963 *J. Phys. Chem. Solids* **24**, 823.

Pant, D. D. 1944 *Proc. Indian Acad. Sci.* A **19**, 315.

Pearlstein, E. A. & Sutton, R. B. 1950 *Phys. Rev.* **79**, 907.

Pogodaev, K. N. 1961 *Sov. Phys. Solid St.* **2**, 1317.

Redfield, A. G. 1954 *Phys. Rev.* **94**, 526.

Robertson, R., Fox, J. J. & Martin, A. E. 1934 *Phil. Trans.* A **232**, 463.

Taylor, K. W. 1956 Thesis, London.

Urlau, R. R. 1960 Thesis, Univ. of the Witwatersrand.

Urlau, R. R., Logie, H. J. & Nabarro, F. R. N. 1961 *Proc. Phys. Soc.* **78**, 256.

Vermeulen, L. A. 1967 *Math. Gaz.* (to be published).

Wedepohl, P. T. 1957 *Proc. Phys. Soc.* B **70**, 177.

Willardson, R. K. & Danielson, G. C. 1950 U.S.A.E.C. ISC-163.